

Oxidation of epitaxial Ce films

E. Vescovo and C. Carbone

Institut für Festkörperforschung des Forschungszentrums Jülich, D-52425 Jülich, Germany

(Received 17 April 1995)

Single-crystal Ce films of more than 300 Å thickness have been epitaxially grown on W(110). Their interaction with molecular oxygen at room temperature has been studied by angle-resolved photoemission, low-energy electron diffraction, and Auger spectroscopy. As a function of the oxygen exposure, the reaction is found to proceed through a sequence of three distinct stages: (i) ordered dissociative surface adsorption; (ii) formation of an ordered Ce₂O₃-like surface oxide; and (iii) gradual conversion of the sesquioxide into a disordered surface dioxide CeO_{2-x}. A structurally different Ce₂O₃ oxide is obtained after high oxygen exposures followed by heating at 450 K. The formation of the epitaxial surface sesquioxides is favored by the good lattice match with the Ce substrate. The same type of structural relation might lead to the formation of ordered sesquioxides on other rare-earth surfaces exposing hexagonal planes.

I. INTRODUCTION

The elementary step in the study of the oxygen interaction with a solid surface is the investigation of the reaction with a well-defined single-crystal surface. This permits us to clarify the relation between the surface reaction and the microscopic structure. In fact, the oxidation of most metals has already been extensively studied on single-crystal surfaces. However, the surface chemistry of rare-earth single crystals has been until now very little investigated because of the difficulties encountered in preparing clean and well-ordered samples.

In the following we report on the oxidation of a single-crystal γ -Ce(111) surface. Metallic Ce has properties that distinguish it from the later elements of the rare-earth series.¹ In Ce, and only to a significantly smaller degree in the two following elements (Pr and Nd), the radial extension of the 4*f* levels is such that their direct hybridization with the nearest neighbors contributes in a non-negligible way to the chemical bonding.² In spite of this fact, investigations of polycrystalline samples show that, when exposed to the simplest and most common molecules, the Ce surface interaction is similar to that of most rare-earth elements.³

The initial stage of the oxidation of polycrystalline Ce has been identified by photoemission,^{4,5} Auger, and electron energy-loss studies,⁶ as the immediate formation of a Ce₂O₃ sesquioxide phase. At higher exposures an oxide layer is formed containing CeO₂. However, the CeO₂ layer grown on the Ce substrate is not stable in ultrahigh-vacuum conditions, but it tends to reconvert into Ce₂O₃. This is remarkable if one considers that CeO₂ is the stable bulk oxide in normal conditions. The oxidation of a Ce single crystal exposing the (100) face has been investigated by electron energy loss.⁶ Also, in this case, the reaction between the oxygen atoms and the Ce surface proceeds in a similar way: sesquioxide nucleation and growth, followed by the formation of a CeO₂-like phase under high oxygen exposures. On the Ce(001) surface, the low-energy electron diffraction (LEED) pattern disappears already after 2-L oxygen exposure. The rapid decrease of the work function seems to indicate oxygen penetration into the subsurface positions right

from the beginning of the oxygen-Ce(001) surface interaction.

In this paper we report on the oxidation of a single-crystal Ce film, epitaxially grown on W(110). Its interaction with molecular oxygen has been studied by angle-resolved photoemission with synchrotron radiation, low-energy electron diffraction, and Auger spectroscopy. We show that the room-temperature oxidation of the crystalline epitaxial Ce films proceeds through a sequence of three very distinct oxidation stages: (1) ordered dissociative surface adsorption up to 1-L exposure; (2) formation of an ordered Ce₂O₃-like surface oxide between 1- and 20-L exposure, and (3) gradual conversion of the sesquioxide into a surface dioxide CeO_{2-x} with loss of long-range order, for oxygen exposures higher than 20 L. Moreover, we report on the observation of a second and structurally different epitaxial film of Ce₂O₃ surface oxide, obtained after high oxygen exposure followed by annealing. The formation and the stability of these epitaxial surface oxides is favored by the good lattice match between the γ -Ce(111) substrate and the Ce₂O₃ bulk oxide. As will be shown, this could have implications also for the oxidation process of other rare-earth metals.

II. EXPERIMENT

The experiment has been performed with an angle-resolved photoemission apparatus on the BESSY TGM-5 wiggler-undulator beamline.⁷ A more complete description of the experimental system has been already reported.⁸ Ce epitaxial overlayers (about 100 atomic layers thick) have been prepared *in situ* on a W(110) surface. Ce has been deposited on the substrate at room temperature by *e*-beam evaporation. The base pressure ($<10^{-10}$ mbar) increased to 2×10^{-10} mbar during Ce evaporation. After evaporation the Ce film is not ordered on the W(110) substrate but a sharp hexagonal LEED pattern is obtained after annealing at 600 K for 1 min. The sample cleanliness has been checked by Auger and photoemission spectroscopy. The latter is very sensitive to small amount of contaminants, as will be shown in the following. We estimate the initial oxygen contamination to be below 1%. The hexagonal LEED pattern, displayed by the annealed

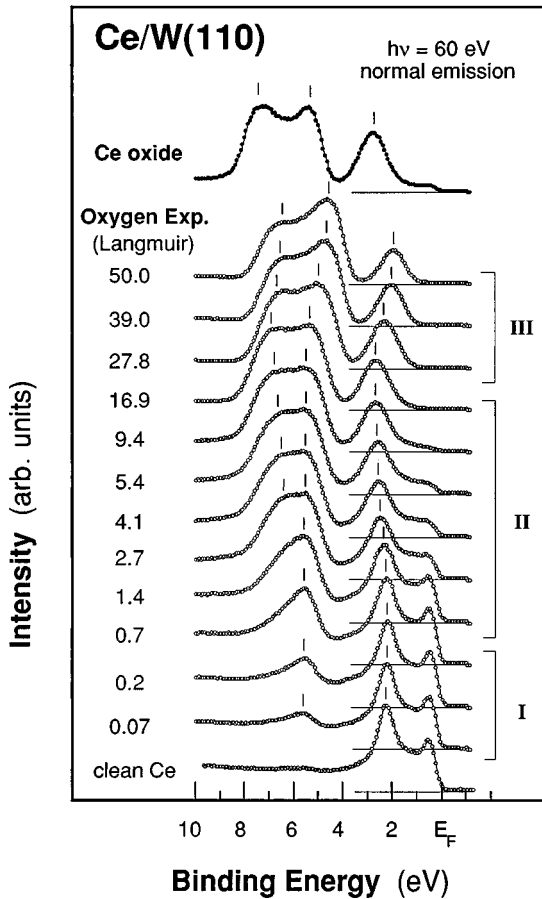


FIG. 1. Normal-emission valence-band spectra of a clean and ordered Ce film deposited on W(110), and during a sequence of oxygen exposures. On top is shown the spectrum (full circles) obtained after exposing the Ce film to 50 L oxygen followed by annealing at 450 K for 10 min.

Ce film, corresponds to the (111) face of a fcc bulk lattice,⁹ with the Ce $[1\bar{1}0]$ axis aligned to the W $[100]$ axis (Nishiyama-Wassermann orientation). This growth mode has been also found for Ce when deposited on V(110).¹⁰ However, on the basis of our LEED information, we cannot exclude that the Ce layer acquires a stacking of the hexagonal planes more complicated than the simple fcc sequence. Crystal structures such as the hcp or the dhcp, which are adopted by other rare earths, are similar, differing from each other and from the fcc lattice only for the stacking sequence of the hexagonal planes. The photoemission spectra have been measured by means of a 90° spherical analyzer. In normal emission conditions, the polarization of the light was parallel to the $\langle 110 \rangle$ direction of the W substrate.

III. RESULTS AND DISCUSSION

Photoemission spectra measured for normal electron emission at 60 eV photon energy as a function of oxygen exposure are presented in Fig. 1. The spectra show clear modifications in correspondence to each of the oxidation stages. The changes in the binding energy and in the relative intensity of the spectral features are for convenience summarized in Figs. 2 and 3, respectively.

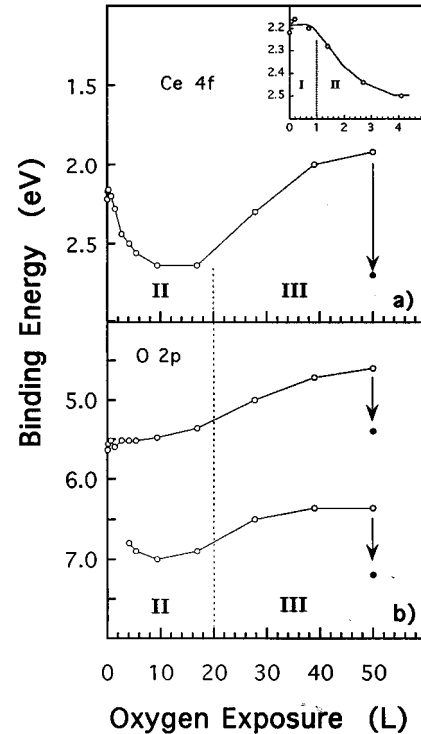


FIG. 2. Plot of the binding-energy positions of the main Ce 4f peak (a) and of the O 2p structures (b) vs oxygen exposure. The full circles refer to the values for the Ce film annealed after an oxygen exposure of 50 L. The inset is an expanded view of the low-oxygen-exposures region.

The clean Ce spectrum shows two structures, one located at the Fermi level and the other at about 2 eV from E_F . These two peaks are mostly due to the emission from the 4f levels, with only a small additional contribution from the $6s5d$ valence-band states in the region close to the Fermi level.¹¹ The binding energy and relative intensity of these two features are very similar to those of γ -Ce spectra.¹¹ The valence-band spectrum of clean Ce does not display other structures in this experimental conditions. Notice that the weak structure at 6 eV binding energy is most likely due to contamination, which we estimate to be below 1%.

From Fig. 1 it appears that up to about 1 L the main change in the photoemission spectra is due to the appearance of a single peak at 5.5 eV binding energy, mostly due to the O 2p emission. This peak displays a very weak dispersion with the emission angle (not shown). At small oxygen coverage (oxygen exposures < 1 L), the oxygen atoms are still far apart and consequently form very narrow bands. During this first stage, the Ce 4f peaks are essentially unchanged with respect to both their binding energy position [Fig. 2(a) inset] and their relative intensity [Fig. 3(a) inset]. Consistently, also the Ce 5p core levels (not shown) are only little modified by the small amount of oxygen deposited on the surface at this level. We interpret this phase of the oxidation process as dissociative surface adsorption. A visual inspection of the LEED pattern reveals that up to this point the pattern is practically identical to the one of the clean Ce(111) substrate. In particular no new superstructure is observed. This indicates that the oxygen atoms adsorb in registry on the γ -Ce(111) face.

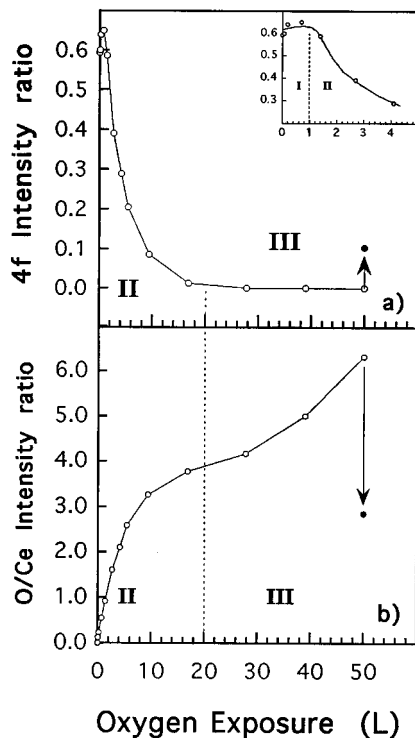


FIG. 3. (a) Plot of the intensity ratio between the Ce 4f photoemission peaks, at the Fermi level and at about 2 eV binding energy, as a function of the oxygen exposure. The inset is an expanded view of the low-oxygen-exposures region. (b) Plot of the exposure-to-cerium signal as derived from the valence-band spectra presented in Fig. 1. The full circles refers to the values for the Ce film annealed after an oxygen exposure of 50 L.

The second stage of the oxidation can be approximately located in the range of oxygen exposure between 1 and 20 L. Major changes are observed in the valence-band photoemission spectra from about 1- to 10-L oxygen exposures (Fig. 1); whereas, from about 10 to 20 L, the position of the peaks does not change appreciably (see also Fig. 2) and the O/Ce intensity ratio tends to saturate [Fig. 3(b)]. The 4f peak located at about 2 eV in the clean Ce metal remains very intense, but it displays a gradual shift toward higher binding energies [Fig. 2(a)] and becomes broader. At the same time, the Ce emission close to the Fermi level sensibly decreases [Fig. 3(a)]. The behavior of the 4f emission is indicative of a depletion of the 5d6s-derived conduction band, with consequent charge transfer into an O 2p-dominated valence band. The depletion of the metal conduction band decreases the screened 4f emission near E_F , thereby determining the observed transfer of weight between the two 4f structures. Notice that the 4f peak remains very intense, indicating the formation of a trivalent surface oxide in which the Ce³⁺ has the 4f¹ configuration.

During this second stage the oxygen 2p-derived emission grows in intensity and develops a two-peaked structure, with broad features located at 5.5 and 7 eV, respectively. This suggests that the oxygen atoms are now sufficiently coordinated with each other to form well-developed 2p bands.

At this point it is useful to compare our photoemission spectra with those reported in the literature for various Ce

oxides.¹² We find that the features of our spectra for 9.4 or 16.9 L closely correspond to those of Ce₂O₃ (Ref. 12) with respect to both energy position and relative intensities. We conclude that the formation of the surface oxide begins above 1 L and converges to a Ce₂O₃-like phase above 10 L.

During this second stage, a sharp hexagonal LEED pattern is still maintained, indicating the formation of an *ordered* surface oxide. The observation of a hexagonal LEED pattern is consistent with the identification of the surface oxide as a Ce₂O₃-like phase. The bulk Ce sesquioxide crystallizes into an hexagonal geometrical structure that can be viewed as a simple stack of planes consisting of Ce atoms or of O atoms.¹³ Inside each plane the Ce (or the O) atoms are arranged in a two-dimensional hexagonal lattice slightly expanded with respect to the one of the γ -Ce(111) ($a_{\text{hex}}^{\text{Ce}_2\text{O}_3} = 3.89 \text{ \AA}$; $a_{\text{hex}}^{\text{Ce}} = 3.65 \text{ \AA}$; with about 6% mismatch). For oxygen exposures up to 20 L, the γ -Ce(111) surface lattice thus stabilizes a Ce₂O₃-like surface oxide with a slightly compressed in-plane hexagonal lattice. A characteristic of the Ce₂O₃ structure is that Ce planes are always sandwiched between two O planes. Our data show that this type of configuration with O planes both below and above the Ce plane should be obtained for oxygen exposures > 10 L. Moreover, this oxide forms a continuous surface layer, as is demonstrated by the attenuation in the photoemission spectra of the Ce substrate signal, which vanishes for exposures > 10 L.

For oxygen exposures above 20 L; the peaks in the photoemission spectra shift in the opposite direction (Fig. 1). This inversion is indicative of a third stage in the oxygen reaction with the Ce surface. The 4f peak moves back to lower binding energy [Fig. 2(a)]. A shift in the same direction is also observed for the oxygen 2p emission [Fig. 2(b)]. Moreover, the relative intensity of these features continue to change. The 4f peak progressively decreases its intensity, indicating a charge transfer from the localized 4f states into the valence band of the oxide; i.e., the trivalent Ce₂O₃ oxide is now gradually converged into the tetravalent CeO₂ oxide. The 4f emission does not disappear completely, indicating that the conversion process to CeO₂ is not complete. The additional fact that the binding energy of the 4f peak continuously changes with increasing oxygen exposure suggests that oxides, with an intermediate oxidation state between Ce₂O₃ and CeO₂ are present in this third oxidation stage. During this third stage, the long-range order is lost, as demonstrated by the rapid deterioration of the LEED pattern, which disappears above 30-L oxygen exposure. For these reasons we attribute this stage to the formation of a disordered surface dioxide of the CeO_{2-x} type.

As already mentioned, the system maintains long-range order for oxygen exposures up to the second stage. However, even at high oxygen coverages, it is possible to recover an ordered structure by heating the system. After the LEED has vanished upon exposure of the Ce film to 50 L oxygen, a sharp hexagonal LEED pattern can be restored by annealing the sample at 450 K for about 10 min. The valence-band photoemission spectrum of the annealed sample is reported at the top of Fig. 1 (full circles). Clearly, all the spectral features are strongly modified by heating. The energy position and the relative intensity of both the Ce 4f and O 2p

emission are similar to those previously observed for the Ce_2O_3 -like surface oxide. This is also apparent from the plots reported in Figs. 2 and 3, where the full circles belong to this annealed system. Furthermore, the Auger spectra also shows that annealing the Ce film exposed to 50 L oxygen restores an oxygen to cerium ratio very close to the one observed in the correspondence to the formation of the Ce_2O_3 oxide. With respect to the Ce_2O_3 -like surface oxide obtained at room temperature, the photoemission spectrum from the annealed oxide shows a weak emission near the Fermi level and O $2p$ peaks more sharp and slightly shifted at higher binding energy. The emission near E_F could originate either from a small amount of uncovered Ce substrate or from a small amount of surface segregated Ce metal on top of the oxide layer. In this second case, from the intensity of the $4f$ emission, we can estimate that the segregated Ce metal would be at most 0.15 ML.

The hexagonal LEED pattern recovered after the heating is slightly contracted with respect to the one of the clean Ce surface, indicating that this second Ce_2O_3 oxide has an in-plane hexagonal lattice that is expanded with respect to the Ce_2O_3 surface oxide formed at room temperature for lower oxygen exposures. Probably, at high temperature, the Ce_2O_3 surface layer relaxes in its stable bulk configuration, which has an in-plane hexagonal lattice expanded with respect to the γ -Ce(111) lattice. The Ce_2O_3 layer so produced is also a rather continuous layer, as is proved by the weakness of the emission near E_F from the metallic Ce in the photoemission spectra.

The angular dependence of the photoemission spectra for this Ce_2O_3 oxide is reported in Fig. 4. The spectra show that the oxygen $2p$ -derived bands display a clear dispersion varying k_{\parallel} along the $\Gamma'X'$ high-symmetry line of the surface Brillouin zone. On the opposite, the atomiclike character of the $4f$ states is reflected in the absence of any dispersion of the $4f$ peak with the emission angle. A summary of the binding-energy positions of the photoemission features of this second Ce_2O_3 oxide versus k_{\parallel} is reported in Fig. 5 (full circles). These data show that the width of the O $2p$ -derived bands of the sesquioxide is about 2 eV. In Fig. 5, at Γ' , we also report the binding energies of the oxygen peaks as derived from the normal emission spectra ($k_{\parallel}=0$) taken at various photon energies from 25 to 60 eV (open circles). In the perpendicular direction the oxygen-dominated bands display a weak dispersion (0.25 eV), which indicates the three-dimensional character of the electronic structure of this epitaxial oxide layer.

IV. COMPARISON WITH OTHER STUDIES

Our study of the oxygen interaction with a single-crystal γ -Ce(111) surface permits us to identify a sequence of three distinct stages in the oxidation reaction and, especially, it shows that the formation of the Ce_2O_3 sesquioxide proceeds without loss of long-range order. At this point, it is useful to discuss our results also in comparison with earlier studies of the oxidation of Ce surfaces.^{3,5,6}

In our experiments, the existence of a dissociative adsorption stage, which precedes the formation of the sesquioxide, is clearly established by recording the photoemission spectra from the localized $4f$ states, which do not show appreciable

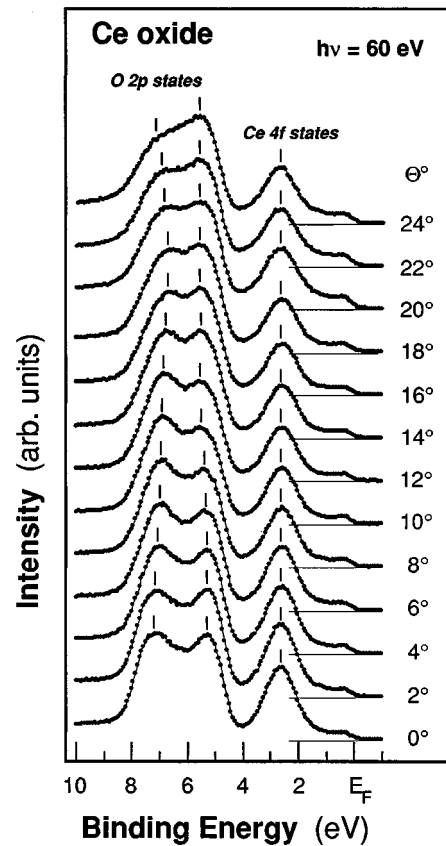


FIG. 4. Off-normal photoemission spectra of the Ce_2O_3 epitaxial oxide layer obtained after exposing the Ce film to 50 L oxygen followed by annealing. The spectra have been measured at room temperature with 60-eV photon energy.

modifications for oxygen exposures <1 L within the accuracy of our measurements. Notice that in a related photoemission study of the oxidation of the Gd(0001) surface,¹⁴ we could detect modifications of the $4f$ peak line shape already for oxygen exposures as low as 0.15 L. Similarly,

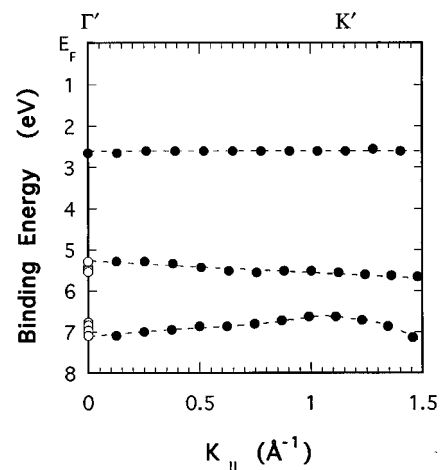


FIG. 5. $E(k_{\parallel})$ values derived from the off-normal data shown in Fig. 4. At Γ' the open circles mark the binding-energy positions of the oxygen peaks in normal-emission spectra taken at various photon energies.

changes of the $4f$ emission have also been shown¹⁵ in some Ce compounds for oxygen exposures below 0.2 L. Possibly, in the case of the Ce(111) surface, high-resolution measurements could reveal modifications of the two peaks near E_F that are not resolved in the present study. Furthermore, the electron-energy-loss-spectroscopy (EELS) spectra of the polycrystalline as well as of Ce(100) surface display already substantial changes at comparable oxygen exposures.^{3,6} However, these changes in the EELS spectra are probably related to the modification of the surface electronic structure of the Ce metal upon oxygen adsorption. During the chemisorption stage, the surface charge of the delocalized $5d6s$ valence electrons on the Ce surface is likely to be modified by the bonding to the adsorbed oxygen atoms.

At higher oxygen exposures, the sesquioxide nucleation and growth is invariably observed in all room-temperature oxidation studies of the Ce surfaces: on the Ce(111) surface (this experiment), as well as on the Ce(001) surface⁶ and on the polycrystalline surface.^{3,6} Furthermore, it is interesting to note that, on V(110), epitaxial Ce_2O_3 films have been obtained by depositing Ce from a not sufficiently outgassed source.¹⁰ This procedure is not well defined and therefore is difficult to reproduce. However, before this work, no observation has been reported on the room-temperature formation of an *ordered* sesquioxide film on the Ce metal. The formation of an epitaxial sesquioxide layer appears favored by the good in-plane lattice match and can probably be observed only oxidizing the (111) hexagonal face of the Ce metal. Nevertheless, the microscopic description of the oxidation reaction might be very similar also for polycrystalline Ce films that preferentially expose the close-packed (111) face. This implies that the structural relation between the metal substrate and the sesquioxide is likely to play a role also in the development of the oxygen reaction with polycrystalline surfaces.

For very heavy oxygen exposure of the polycrystalline surface, the formation of the tetravalent CeO_2 oxide has been also observed.^{3,5,6} Moreover, it has been noticed⁵ that, at room temperature in ultrahigh-vacuum condition, this surface oxide is metastable because, with time, it reconverts into Ce_2O_3 . Similarly, in our experiment on the γ -Ce(111) substrate, it has been shown that the sesquioxide can be reobtained from CeO_{2-x} by annealing the system. Furthermore, in the formation of this new Ce_2O_3 layer, the long-range order is also recovered. These facts indicate that the stability of the sesquioxide might be closely related to the good lattice match of the hexagonal planes of sesquioxide and the Ce metal. On the other side, the fact that in the case of the Ce(100) surface it has also been found⁶ that, at room temperature, the CeO_2 stoichiometry could be maintained on the surface only by means of a stationary oxygen pressure $>10^{-8}$ Torr, shows that the lattice match condition is only one of the many parameters that determine the development of the surface reaction.

Finally, we would like to mention that, although it is well known that the room-temperature oxidation of most rare-

earth metals (R) leads to the formation of the sesquioxides (R_2O_3)³, to our knowledge no observation of *ordered* R_2O_3 layers has been reported before this work. We believe that the formation of well-ordered surface sesquioxides with the hexagonal structure can be quite a general step in the oxidation of rare-earth crystals exposing hexagonal faces [e.g., fcc-(111); hcp-(0001)]. The formation of ordered sesquioxide is indeed most probable for the light rare-earth metals (La, Pr, Nd). Their sesquioxides have in fact the same hexagonal structure of Ce_2O_3 . The same type of structural relation found between Ce and its sesquioxide holds true also for them (for $M = La, Pr, Nd$: a_{hex}^M is 3.75, 3.67, and 3.66 Å and $a_{hex}^{M_2O_3}$ is 3.94, 3.86, and 3.83 Å, which imply 5.0%, 5.1%, and 4.6% lattice mismatch, respectively). Furthermore, even rare earths, whose stable sesquioxides do not crystallize into a simple stack of hexagonal planes, might still form hexagonal surface sesquioxides. For example, on a thick Gd(0001) film epitaxially grown on W(110), it has been found¹⁶ that a simple hexagonal LEED pattern is maintained up to very high oxygen exposures at room temperature. Furthermore, the hexagonal LEED is very stable because it does not change either by annealing the system up to temperatures of 500 °C or by exposing the system to the atmosphere for 1 h. These LEED observations are very surprising because they cannot be explained by means of the cubic structure of bulk Gd_2O_3 .¹⁶ The persistence of a simple hexagonal pattern has been interpreted as due to the adsorption of a passivating O layer, which does not alter the geometrical structure of the underlying metal layers.¹⁶ In view of our results an alternative explanation is instead that, similarly to the Ce(111) case, the hexagonal Gd(0001) surface lattice stabilizes a surface sesquioxide with a hexagonal structure.

V. CONCLUSIONS

In conclusion, we have studied the oxygen interaction with single-crystal Ce films, epitaxially grown on W(110). Upon oxygen exposure, three different stages can be distinguished: an ordered dissociative oxygen adsorption stage up to 1 L; the formation of an ordered trivalent Ce_2O_3 -like oxide in the region between 2 and 20 L; and the gradual conversion of this trivalent oxide layer into a disordered tetravalent CeO_2 one, for higher oxygen exposures. A second ordered Ce_2O_3 oxide layer can be obtained by annealing the sample after high oxygen exposures. This second type of Ce_2O_3 oxide displays an in-plane hexagonal lattice expanded with respect to the one of the γ -Ce(111). The growth of ordered sesquioxides on the hexagonal γ -Ce(111) substrate is explained by the good in-plane lattice match conditions.

ACKNOWLEDGMENTS

We wish to thank W. Eberhardt and W. Gudat for their interest in this work and for their continuous support. We are also indebted to D. D. Sarma for fruitful discussions.

- ¹J. W. Allen, S. J. Oh, O. Gunnarsson, K. Schönhammer, M. B. Maple, M. S. Torikachvili, and I. Lindau, *Adv. Phys.* **35**, 275 (1986).
- ²Y. Baer, in *Handbook on the Physics and Chemistry of Rare Earths*, edited by K. A. Gschneider, Jr., L. Eyring, and S. Hufner (Elsevier, Amsterdam, 1986), Vol. 10, p. 1.
- ³F. P. Netzer and J. A. D. Matthew, *Rep. Prog. Phys.* **49**, 621 (1986); F. P. Netzer and E. Bertel, in *Handbook on the Physics and Chemistry of Rare Earths* (Ref. 2), Vol. 5, p. 217.
- ⁴A. Platau, L. I. Johansson, A. L. Hagström, S. E. Karlsson, and S. B. M. Hagström, *Surf. Sci.* **63**, 153 (1977); A. Platau and S.-E. Karlsson, *Phys. Rev. B* **18**, 3820 (1978).
- ⁵D. D. Sarma, M. S. Hegde, and C. N. R. Rao, *J. Chem. Soc. Faraday Trans. 2* **77**, 1509 (1981).
- ⁶G. Strasser, G. Rosina, E. Bertel, and F. P. Netzer, *Surf. Sci.* **152/153**, 765 (1985).
- ⁷W. Peatman, C. Carbone, W. Gudat, W. Heinen, P. Kuske, J. Pflüger, F. Schäfers, and T. Schroeter, *Rev. Sci. Instrum.* **60**, 1445 (1989).
- ⁸E. Kisker and C. Carbone, in *Angle-Resolved Photoemission*, edited by S. Kevan (Elsevier, Amsterdam, 1992).
- ⁹E. Weschke, A. Höhr, C. Laubschat, and G. Kaindl (unpublished).
- ¹⁰B. Kierren, T. Gourieux, F. Bertran, and G. Krill, *Phys. Rev. B* **49**, 1976 (1994).
- ¹¹D. Wieliczka, J. H. Weaver, D. W. Lynch, and C. G. Olson, *Phys. Rev. B* **26**, 7056 (1982).
- ¹²E. Wuilloud, B. Delley, W.-D. Schneider, and Y. Baer, *Phys. Rev. Lett.* **53**, 202 (1984); J. W. Allen, *J. Magn. Magn. Mater.* **47/48**, 168 (1985); S. Hufner, in *Handbook on the Physics and Chemistry of Rare Earths* (Ref. 2), Vol. 10, p. 301.
- ¹³L. Pauling, *Z. Kristallogr.* **69**, 415 (1929); D. J. M. Bevan and T. M. Height, in *Handbook on the Physics and Chemistry of Rare Earths* (Ref. 2), Vol. 3, p. 342; H. Bärnighausen and G. Schiller, *J. Less-Common Met.* **110**, 385 (1985).
- ¹⁴E. Vescovo, O. Rader, T. Kachel, U. Alkemper, and C. Carbone, *Phys. Rev. B* **47**, 13 899 (1993).
- ¹⁵R. I. R. Blyth, A. B. Andrews, A. J. Arko, J. J. Joyce, P. C. Canfield, Z. Fisk, U. G. L. Lahiase, and L. DeLong, *Surf. Rev. Lett.* **4**, 565 (1994).
- ¹⁶D. Weller and D. D. Sarma, *Surf. Sci.* **171**, L425 (1986).